



PII: S0364-5916(03)00035-X

DOI: 10.1016/S0364-5916(03)00035-X

**Thermodynamic Description of the Cu-Al-Mn System in the Copper-Rich Corner**

J. Miettinen

Laboratory of Metallurgy, Vuorimiehentie 2K

Helsinki University of Technology, FIN-02015 HUT, Finland

E-mail: jyrki.miettinen@hut.fi

(Received January 24, 2003)

**Abstract** Thermodynamic description of the ternary Cu-Al-Mn system in its copper-rich corner is presented. The thermodynamic parameters of the sub-systems, Cu-Al, Cu-Mn and Al-Mn, are taken from earlier SGTE-based assessments (after modifying the Cu-Mn description slightly) and those of the ternary Cu-Al-Mn system are optimized in this study by using the experimental phase equilibrium data. The present ternary description is valid for aluminum contents up to 18 wt% and manganese contents up to 50 wt%. © 2003 Published by Elsevier Science Ltd.

**Introduction**

In the present study, a thermodynamic description is presented for the Cu-Al-Mn system in its copper-rich corner. Thermodynamic data are optimized for the system using the earlier assessed data of binaries Cu-Al [98Ans, 02Mie1], Cu-Mn [96Vre] (partly reassessed in this study) and Al-Mn [98Ans], and applying the experimental phase equilibrium data of the literature. The study continues the recently started work for the development of a thermodynamic database for technically important copper alloys (Table 1).

TABLE 1

Ternary systems Cu-X-Y of the copper alloys database. Earlier assessed systems are indicated by a reference code and those to be assessed within the next few years are indicated by F (future work).

X \ Y	Fe	Mn	Ni	Si	Sn	Zn	P
Al	03Mie	this study	F	F	02Mie1	02Mie2	
Fe		F	87Jan	F			
Mn			F	F	F	F	
Ni				F	F	F	
Si						F	
Sn						02Mie2	01Mie

**Phases and Models**

Fig.1 shows the calculated phase diagrams for binaries Cu-Al [02Mie1] and Al-Mn [98Ans]. They agree well with the experimental phase equilibrium data as shown in these studies.

The phase equilibria of the Cu-Al-Mn system have been reviewed by Chang *et al.* [79Cha] and Lukas [98Luk]. In the present description, valid in the copper-rich corner of the system, the following phases are considered: liquid, fcc, bcc, gamma, cbcc ( $\alpha$ Mn), cub ( $\beta$ Mn) and  $\text{Cu}_3\text{Mn}_2\text{Al}$  ( $\tau$ ). The disordered solution phases, liquid, fcc, bcc, cbcc and cub are described with the substitutional solution model and the  $\tau$  phase, assumed stoichiometric, is described with the sublattice model. Also, the ordered gamma phase is described with the substitutional solution model, due to the earlier chosen strategy to apply the substitutional solution model to any type of gamma phase [02Mie1, 02Mie2]. This strategy was adopted due to the complexity of the sublattice treatment for cases where the gamma phase structures of the binary sub-systems are different. It is

worth noting that the disorder-order transitions of the bcc phase, from A2 to B2, D0<sub>3</sub> and L2<sub>1</sub> [98Kai] are not considered in the present study. This is due to the lack of the proper thermodynamic descriptions from the Cu-Al system [98Ans, 02Mie1].

By applying the substitutional solution model to the solution phases of the Cu-Al-Mn system, the molar Gibbs energy of these phases becomes

$$G_m^\phi = x_{Al}^\phi \text{}^oG_{Al}^\phi + x_{Cu}^\phi \text{}^oG_{Cu}^\phi + x_{Mn}^\phi \text{}^oG_{Mn}^\phi + RT(x_{Al}^\phi \ln x_{Al}^\phi + x_{Cu}^\phi \ln x_{Cu}^\phi + x_{Mn}^\phi \ln x_{Mn}^\phi) + x_{Al}^\phi x_{Cu}^\phi L_{Al,Cu}^\phi + x_{Al}^\phi x_{Mn}^\phi L_{Al,Mn}^\phi + x_{Cu}^\phi x_{Mn}^\phi L_{Cu,Mn}^\phi + x_{Al}^\phi x_{Cu}^\phi x_{Mn}^\phi L_{Al,Cu,Mn}^\phi + \text{}^mG_m^\phi \quad (1)$$

where the contribution to the Gibbs energy due to the magnetic ordering,  $\text{}^mG_m^\phi$ , is expressed as

$$\text{}^mG_m^\phi = RT \ln(\beta^\phi + 1) \cdot f(\tau) \quad (2)$$

In Eq. (1), R is the gas constant (8.3145J/Kmol), T is the absolute temperature,  $x_i$  is the mole fraction of component i,  $\text{}^oG_i^\phi$  is the Gibbs energy of pure component i in phase  $\phi$  expressed relative to the enthalpy of the component in its stable phase at 298.15K [91Din],  $L_{ij}^\phi$  is a binary parameter describing the interaction between components i and j in phase  $\phi$ , and  $L_{Al,Cu,Mn}^\phi$  is a ternary interaction parameter of phase  $\phi$ . For these parameters,  $\text{}^oG_i^\phi$  is a function of temperature, and  $L_{ij}^\phi$  and  $L_{Al,Cu,Mn}^\phi$  can be functions of temperature and composition. In Eq. (2),  $\beta^\phi$  is a composition-dependent parameter related to the total magnetic entropy and  $\tau$  is defined as  $\tau=T/T_c^\phi$  where  $T_c^\phi$  is the critical temperature of magnetic ordering. For the bcc and fcc phases, the function  $f(\tau)$  takes the polynomial form proposed by Hillert and Jarl [78Hil]. For the other phases,  $\text{}^mG_m^\phi=0$ .

Phase Cu<sub>3</sub>Mn<sub>2</sub>Al ( $\tau$ ) is described with the sublattice model assuming a complete occupation of the atoms of one component type in each sublattice. The Gibbs energy of formation of the phase is expressed as

$$\text{}^oG_{CuMnAl}^\tau = 0.5 \text{}^oG_{Cu}^{fcc} + 0.333 \text{}^oG_{Mn}^{bcc} + 0.167 \text{}^oG_{Al}^{fcc} + A + BT \quad (3)$$

where  $\text{}^oG_i^\phi$  is the Gibbs energy of pure component i in its stable phase at 298.15K [91Din].

## Experimental Data

Chang *et al.* [79Cha] and Lukas [98Luk] have reviewed the earlier, experimental studies on the Cu-Al-Mn system. Table 2 shows the experimental information selected in the present optimization. The Cu-Mn system is included due to the reassessing of its solid-state data (Section “Results”).

TABLE 2  
Experimental information applied in the optimization process.

System	Experimental information type	Ref.
Cu-Mn	Phase equilibria of the phase diagram Molar Gibbs energy of solid alloys, at 1053K Activity of Mn in solid alloys, at 1070 and 980K	30Smi, 39Gru, 45Dea, 57Hel, 71Sch 69Kre 79Haj
Cu-Al-Mn	Six isotherms, at 950, 800, 700, 600, 550 and 500°C Three isopleths, at $x_{Mn}=0.10, 0.15$ and $0.20$ Enthalpy of formation of solid alloys, at 298K	56Wes, 66Kös, 79Cha (assessed) 56Wes, 98Kai 37Kör

## Thermodynamic Description

The thermodynamic description of the Cu-Al-Mn system is presented in Table 3. The parameters marked with a reference code were adopted from the earlier SGTE assessments and those marked with \*O or \*E were optimized or estimated in the present study. By \*O, the parameter was optimized using the experimental data of literature (Table 2) and by \*E, the parameter was estimated arbitrarily, by applying no experimental data (since not available). The thermodynamic data of the pure components are given by Dinsdale [91Din], except for the

gamma phase and copper in the bcc and cub phases. In the latter case, the Gibbs energy differences of pure copper in the bcc and cub structures relative to the fcc structure were assumed identical to those of pure nickel [91Din], due to the lack of the proper SGTE data for the bcc and cub copper. The magnetic ordering parameters for the fcc and bcc phases are  $\beta^{fcc}=0.62x_{Mn}$ ,  $T_c^{fcc}=540x_{Mn}$ ,  $\beta^{bcc}=-0.27x_{Mn}$  and  $T_c^{bcc}=-580x_{Mn}$  [98Ans]. The presented description is valid up to 18 wt% Al [02Miel] and 50 wt% Mn.

TABLE 3

Thermodynamic data for the Cu-Al-Mn system obtained from the literature (reference code) and optimized (\*O) or estimated (\*E) in this study. All parameter values are in J/mol. The thermodynamic data of the pure components are taken from Dinsdale [91Din] unless a parameter expression is shown in the Table.

<b>liquid</b> (1 sublattice, sites: 1, constituents: Al,Cu,Mn)	<b>Ref.</b>
$L_{Al,Cu}^L = (-66622+8.1T) + (46800-90.8T+10T\ln T)(x_{Al}-x_{Cu}) + (-2812)(x_{Al}-x_{Cu})^2$	98Ans
$L_{Al,Mn}^L = (-66174+27.099T) + (-7509+5.484T)(x_{Al}-x_{Mn}) + (-2639)(x_{Al}-x_{Mn})^2$	98Ans
$L_{Cu,Mn}^L = (1800-2.28T) + (-6500-2.91T)(x_{Cu}-x_{Mn})$	96Vre
$L_{Al,Cu,Mn}^L = -67000+50T$	*O
<b>fcc</b> (1 sublattice, sites: 1, constituents: Al,Cu,Mn)	<b>Ref.</b>
$L_{Al,Cu}^{fcc} = (-64400+10T) + (34000)(x_{Al}-x_{Cu})$	02Miel
$L_{Al,Mn}^{fcc} = (-69300+25T) + (8800)(x_{Al}-x_{Mn})$	98Ans
$L_{Cu,Mn}^{fcc} = (11820-2.3T) + (-10600+3T)(x_{Cu}-x_{Mn}) + (0)(x_{Cu}-x_{Mn})^2 + (-4850+3.5T)(x_{Cu}-x_{Mn})^3$	*O
$L_{Al,Cu,Mn}^{fcc} = 17000$	*O
<b>bcc</b> (1 sublattice, sites: 1, constituents: Al,Cu,Mn)	<b>Ref.</b>
$L_{Al,Cu}^{bcc} = (-104600+27.5T) + (9800+20T)(x_{Al}-x_{Cu})$	02Miel
$L_{Al,Mn}^{bcc} = (-120077+52.851T) + (-40652+29.276T)(x_{Al}-x_{Mn})$	98Ans
$L_{Cu,Mn}^{bcc} = (11190-6T) + (-9865)(x_{Cu}-x_{Mn})$	*O
$L_{Al,Cu,Mn}^{bcc} = 36000$	*O
<b>gamma</b> ( $\gamma$ ) (1 sublattice, sites: 1, constituents: Al,Cu,Mn)	<b>Ref.</b>
${}^0G_{Al}^{\gamma} = {}^0G_{Al}^{fcc} + 10$	98Lia
${}^0G_{Cu}^{\gamma} = {}^0G_{Cu}^{fcc} + 10$	98Lia
${}^0G_{Mn}^{\gamma} = {}^0G_{Mn}^{bcc} + 10$	*E
$L_{Al,Cu}^{\gamma} = (-53150+18.6T) + (236000-27.8T)(x_{Al}-x_{Cu}) + (364000-88.3T)(x_{Al}-x_{Cu})^2$	02Miel
$L_{Al,Mn}^{\gamma} = 50000$ (gamma not stable in binary Al-Mn)	*E
$L_{Cu,Mn}^{\gamma} = 50000$ (gamma not stable in binary Cu-Mn)	*E
$L_{Al,Cu,Mn}^{\gamma} = (-800000)x_{Al} + (-100000+100T)x_{Cu} + (-400000)x_{Mn}$	*O
<b>cbcc</b> (1 sublattice, sites: 1, constituents: Al,Cu,Mn)	<b>Ref.</b>
${}^0G_{Cu}^{cbcc} = {}^0G_{Cu}^{fcc} + 3556$ (data assumed identical to that of pure Ni [91Din])	*E
$L_{Al,Cu}^{cbcc} = 0$ (cbcc not stable in binary Cu-Al)	*E
$L_{Al,Mn}^{cbcc} = -101410+43T$	98Ans
$L_{Cu,Mn}^{cbcc} = 35000$	*O
$L_{Al,Cu,Mn}^{cbcc} = -40000$	*O
<b>cub</b> (1 sublattice, sites: 1, constituents: Al,Cu,Mn)	<b>Ref.</b>
${}^0G_{Cu}^{cub} = {}^0G_{Cu}^{fcc} + 2092$ (data assumed identical to that of pure Ni [91Din])	*E
$L_{Al,Cu}^{cub} = 0$ (cub not stable in binary Cu-Al)	*E
$L_{Al,Mn}^{cub} = (-119022+52.507T) + (-1763)(x_{Al}-x_{Mn})$	98Ans
$L_{Cu,Mn}^{cub} = 35000$	*O
$L_{Al,Cu,Mn}^{cub} = -216000+100T$	*O
<b>Cu<sub>3</sub>Mn<sub>2</sub>Al</b> ( $\tau$ ) (3 sublattices, sites: 0.500:0.333:0.167, constituents: Cu:Mn:Al)	<b>Ref.</b>
${}^0G_{Cu:Mn:Al}^{\tau} = 0.500{}^0G_{Cu}^{fcc} + 0.333{}^0G_{Mn}^{cbcc} + 0.167{}^0G_{Al}^{fcc} + (-13900)$	*O

## Results

In the following, calculated phase diagrams of the binary sub-systems are presented, and calculated results of the Cu-Mn and Cu-Al-Mn systems are compared with the original experimental data to demonstrate the successfulness of the optimization. All calculations were carried out with the ThermoCalc software [85Sun].

### System Cu-Mn

The Cu-Mn system was recently assessed by Vreštal *et al.* [96Vre]. The calculated results agree reasonably well with the measured phase equilibrium [39Gru, 57Hel, 71Sch] and thermodynamic [68Spe, 69Kre, 79Sat, 93Lew, 96Vre] data, when taking into account the inconsistencies in the experimental thermodynamic data. More recently, Dinsdale [00Din] noticed that the bcc phase became stable in the middle of the Cu-Mn diagram, where it should not be. This was corrected by optimizing new bcc phase data for the system. In the present study, not only the bcc phase data but also the data of the other solid phases were reoptimized. Consequently, slightly better agreement was obtained between the calculated and experimental [30Smi, 39Gru, 45Dea, 57Hel, 71Sch, 94Goc] phase equilibria in the system, as shown by the Cu-Mn phase diagram of Fig.2 and the invariant phase equilibria of Table 4. Also, the validity of the new thermodynamic data was checked. As shown by Fig.3, the present and the earlier calculations (when ignoring the falsely calculated bcc region in the latter) agree equally well with the experimental molar Gibbs energy data [69Kre] and the experimental manganese activity data [79Haj] of solid alloys. The liquid phase data of Vreštal *et al.* were adopted as such, since its reoptimization would require more accurate and more consistent thermodynamic data than available from the literature [68Spe, 79Sat, 93Lew, 96Vre].

TABLE 4  
Assessed (experimental) and calculated invariant phase equilibria of the Cu-Mn system.

$\phi 1 - \phi 2 - \phi 3$	T(°C)	$x_{Mn}^{\phi 1}$	$x_{Mn}^{\phi 2}$	$x_{Mn}^{\phi 3}$	Ref.
Liq - bcc - fcc	1100	0.762	0.875	0.885	Exp 94Goc
	1100	0.732	0.892	0.902	Cal This study
	1103	0.734	0.891	0.902	Cal 96Vre
Liq - fcc (congruent point)	873	0.380	0.380		Exp 94Goc
	879	0.380	0.380		Cal This study
	881	0.369	0.369		Cal 96Vre
Fcc - cub - cbcc	725	0.780	0.996	0.997	Exp 94Goc
	704	0.784	0.995	0.996	Cal This study
	707	0.893	1.000	1.000	Cal 96Vre

### System Cu-Al-Mn

Figs. 4 through 9 show six calculated isothermal sections for the Cu-Al-Mn system, at temperatures of 950°C, 800°C, 700°C, 600°C, 550°C and 500°C, respectively. The agreement with the experimental data [56Wes, 66Kös, 79Cha] is relatively good. At temperatures below 950°C, the experimental data shown in the diagrams are from [56Wes] only, but the calculated phase equilibria also agree well with the measurements of [66Kös], though up to manganese contents of about 40 wt% Mn only. For the three invariant reactions containing the  $Cu_3Mn_2Al$  ( $\tau$ ) phase, i.e.,  $bcc+cub \leftrightarrow fcc+\tau$ ,  $bcc+cub \leftrightarrow \gamma+\tau$  and  $bcc \leftrightarrow fcc+\gamma+\tau$ , the temperature values of 520°C, 420°C and 400°C were suggested [66Kös], respectively. As these values were interpolated from a limited amount of experimental data, their agreement with the calculated temperatures, 534°C, 454°C and 393°C, can be considered satisfactory. The phase compositions of [66Kös] deviated from the calculated values with about 1 to 3 wt% of aluminum and manganese. Also the 450°C isotherm was calculated but in this case, the bcc phase was located at slightly lower aluminum contents than shown by the measurements [56Wes]. Consequently, all the bcc phase containing phase equilibrium regions were slightly distorted. Trials were made to correct this, by optimizing composition dependent ternary interaction parameters for the phases, but no clear improvement was achieved.

Three calculated isopleths of the Cu-Al-Mn system, at constant manganese contents of  $x_{Mn}=0.1$ ,  $x_{Mn}=0.15$  and  $x_{Mn}=0.2$ , are presented in Figs. 10 through 12. On the whole, the calculated results agree reasonably well with the experimental data [52Wes, 98Kai].

Finally, Fig.13 shows calculated enthalpy of formation of ternary alloys at 298K, at a composition ratio of Cu:Mn=2. The agreement with the experimental data of Körber *et al.* [37Kör] is quite good.

### Summary

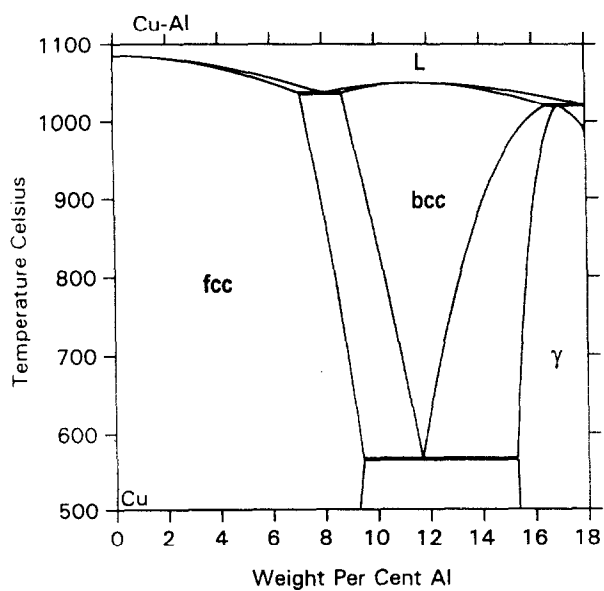
A thermodynamic description was presented for the ternary Cu-Al-Mn system applying the experimental phase equilibrium data of the literature. By limiting the validity of the description to the copper-rich corner, seven phases of the system, i.e., liquid, fcc, bcc, gamma, cbcc, cub and Cu<sub>3</sub>Mn<sub>2</sub>Al ( $\tau$ ), were considered. From these phases, the disordered solution phases, i.e., liquid, fcc, bcc, cbcc and cub, and the ordered gamma phase were described with the substitutional solution model, and the Cu<sub>3</sub>Mn<sub>2</sub>Al ( $\tau$ ) phase, assumed stoichiometric, was described with the sublattice model. In the optimization, the unary and binary thermodynamic data of the system were taken from the recently assessed SGTE descriptions excluding the solid phases of the Cu-Mn system, the data of which were reoptimized in the present study. Good or reasonable correlation was obtained between the calculated and the experimental phase equilibrium data.

### Acknowledgement

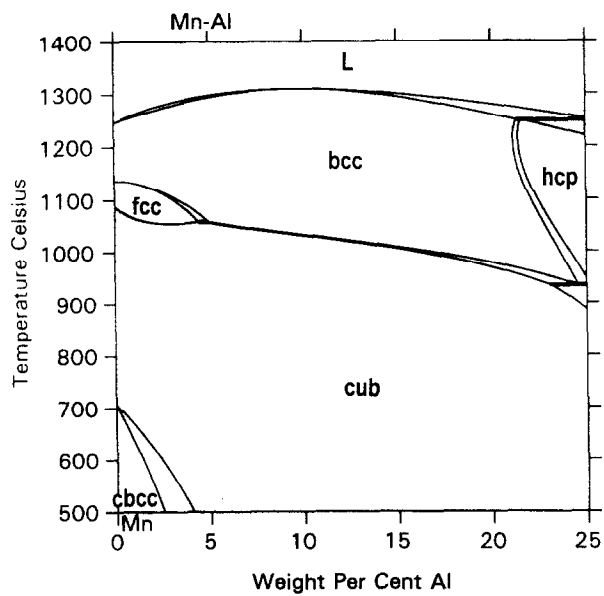
Financial support of Outokumpu Research Oy, Pori, Outokumpu Poricopper Oy, Pori, and the Technology Development Center (TEKES) during the project *Continuous casting of demanding copper alloys* (VAKU) is gratefully acknowledged.

### References

- 30Smi C.S. Smith, *Trans. AIME*, **89** (1930) 164-93.  
 37Kör F. Körber, W. Oelsen and H. Lichtenberg, *Mitt. KWI für Eisenforsch.*, **19** (1937) 131-59.  
 39Gru G. Grube, E. Östereicher and O. Winkler, *Zeit Elektrochem.*, **45** (1939) 776-84.  
 45Dea R.S. Dean, J.R. Long, T.R. Graham, E.V. Potter and E.T. Hayes, *Trans. ASM*, **34** (1945) 443-64.  
 56Wes D.R.F. West and D.L. Thomas, *J. Inst. Metals*, **85** (1956/57) 97-104.  
 57Hel A. Hellowell and W. Hume-Rothery, *Roy. Soc. London-Phil. Trans. Series*, **249** (1957) 417-59.  
 66Kös W. Köster and T. Gödecke, *Z. Metallkd.*, **57** (1966) 889-901.  
 68Spe P.J. Spencer and J.N. Pratt, *Trans. Far. Soc.*, **64** (1968) 1470-76.  
 69Kre R.W. Krenzer and H.J. Pool, *Trans. Met. Soc. AIME*, **245** (1969), 91-98.  
 71Sch E. Schürmann and E. Schulz, *Z. Metallkd.*, **62** (1971) 758-62.  
 78Hil M. Hillert and M. Jarl, *CALPHAD*, **2** (1978) 227-38.  
 79Cha Y.A. Chang, J.P. Neumann, A. Mikula and D. Goldberg, *The Metallurgy of Copper, Phase Diagrams and Thermodynamic Properties of Ternary Copper-Metal Systems*, INCRA Monograph VI, 1979.  
 79Haj J.P. Hajra, *Sripta Met.*, **13** (1979) 173-75.  
 79Sat S. Sato and O.J. Kleppa, *Metall. Trans. B*, **10B** (1979) 63-66.  
 85Sun B. Sundman, B. Jansson and J-O. Andersson, *CALPHAD*, **9** (1985) 153-90.  
 91Din A.T. Dinsdale, *CALPHAD*, **15** (1991) 317-425.  
 93Lew K. Lewin, D. Sichen and S. Seetharaman, *Scand. J. Met.*, **22** (1993) 310-16.  
 94Goc N.A. Gocken, in *Phase Diagrams of Binary Copper Alloys*, P.R. Subramanian, D.J. Chakrabarti and D.E. Laughlin eds., ASM International, Materials Park, OH, 1994, 253-59.  
 96Vre J. Vrešt'ál, J. Štěpánková and B. Broz, *Scand. J. Metall.*, **25** (1996) 224-31.  
 98Ans I. Ansara, A.T. Dinsdale and M.H. Rand, *COST 507 - Thermochemical database for light metal alloys*, Volume 2, European Communities, Belgium, 1998.  
 98Luk H. Lucas, in *COST 507 - Critical evaluation of ternary systems*, Volume 3, G. Effenberg, ed., European Communities, Belgium, 1998, 51-80.  
 98Kai R. Kainuma, N. Satoh, X. Liu, I. Ohnuma and K. Ishida, *J. Alloys Compounds*, **266** (1998) 191-200.  
 98Lia H. Liang and Y.A. Chang, *J. Phase Equilibria*, **19** (1998) 25-37.  
 00Din A. Dinsdale, Private communication, National Physical Laboratory, Teddington, Middlesex, 2000.  
 01Mie J. Miettinen, *CALPHAD*, **25** (2001) 43-58.  
 02Mie1 J. Miettinen, *Metall. Mater. Trans. A*, **33A** (2002) 1639-48.  
 02Mie2 J. Miettinen, *CALPHAD*, **26** (2002) 119-39.  
 03Mie J. Miettinen, *CALPHAD*, **27** (2003), this issue.



(a)



(b)

FIG.1  
Calculated phase diagrams of binaries Cu-Al (a) and Al-Mn (b).

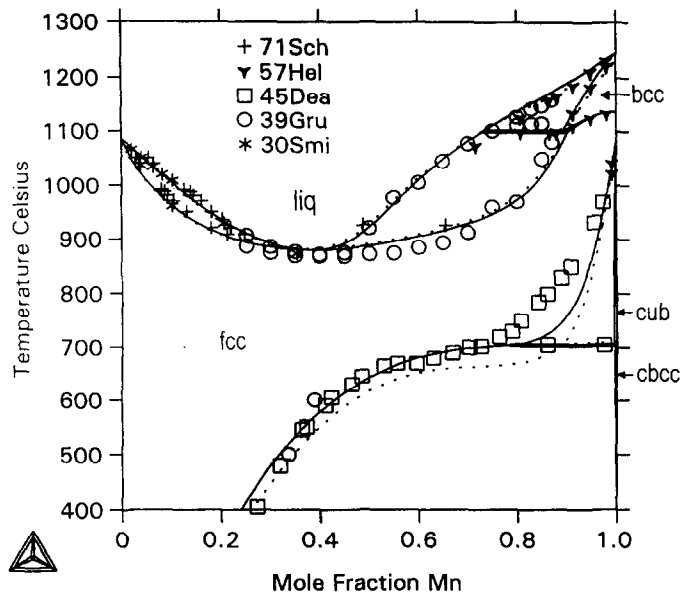


FIG.2

Calculated Cu-Mn phase diagram, together with experimental data points [30Smi, 39Gru, 45Dea, 57Hel, 71Sch]. Solid lines refer to the calculations of this study and dashed lines refer to those of the earlier description [96Vre]. The bcc phase of [96Vre] has been removed from the diagram due to its unreliably strong stability.

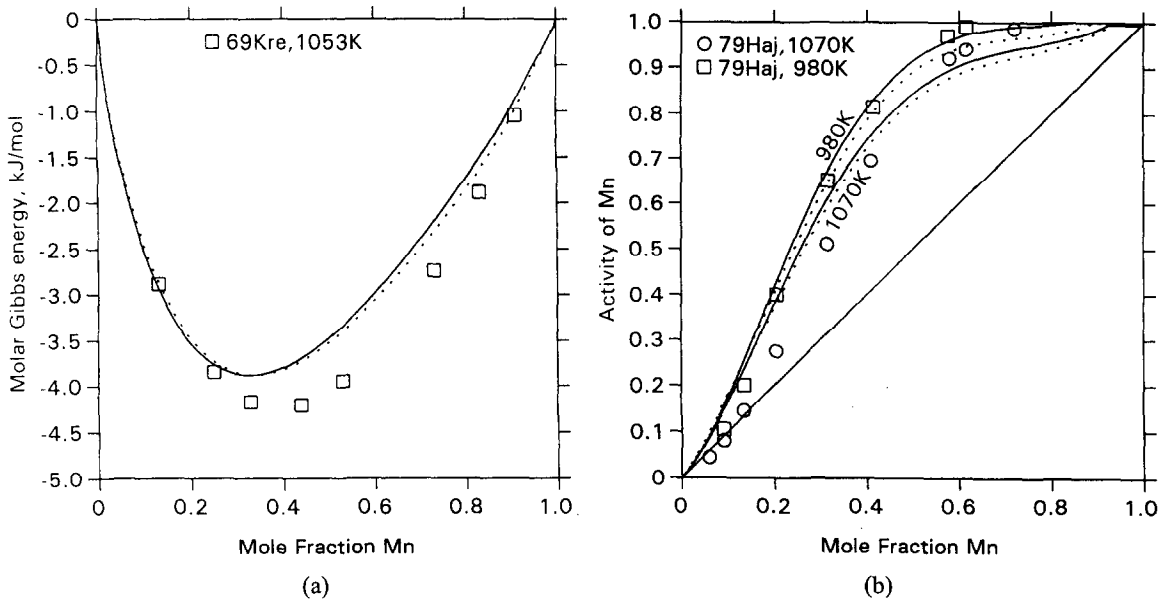


FIG.3

Calculated molar Gibbs energies of solid Cu-Mn alloys at 1053K (a) and activity of manganese in solid Cu-Mn alloys at 1070K and 980K (b), together with experimental data points [69Kre, 79Haj]. Solid lines refer to the calculations of this study and dashed lines refer to those of the earlier description [96Vre]. The reference states for copper and manganese are pure fcc Cu and pure cub Mn, respectively.

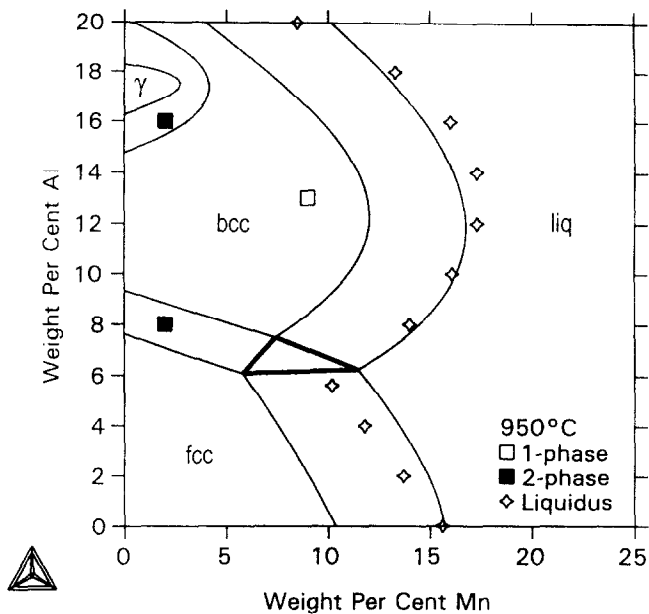


FIG.4

Calculated isothermal section in the copper-rich part of the Cu-Al-Mn system at 950°C, together with experimental data points [66K6s] and the critically reviewed experimental data points of the liquidus [79Cha].

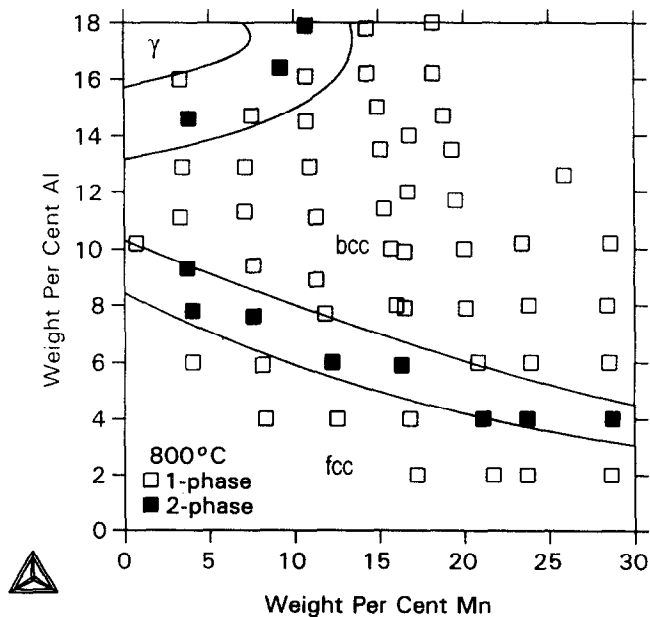


FIG.5

Calculated isothermal section in the copper-rich part of the Cu-Al-Mn system at 800°C, together with experimental data points [56Wes].

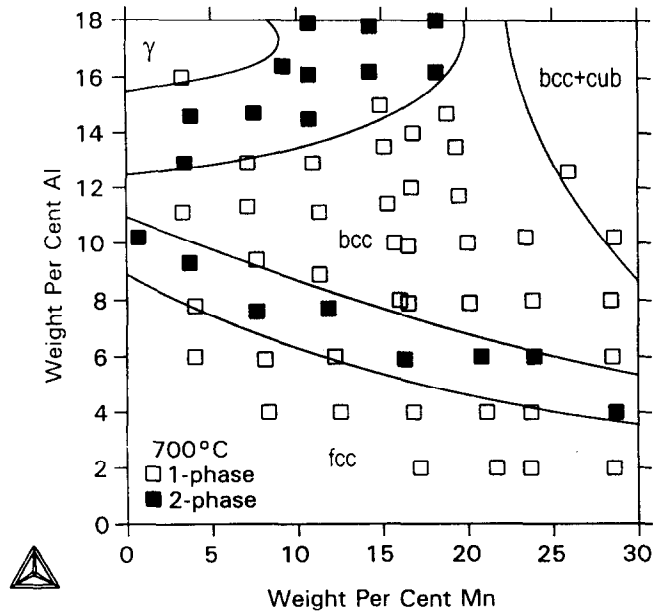


FIG.6

Calculated isothermal section in the copper-rich part of the Cu-Al-Mn system at 700°C, together with experimental data points [56Wes].

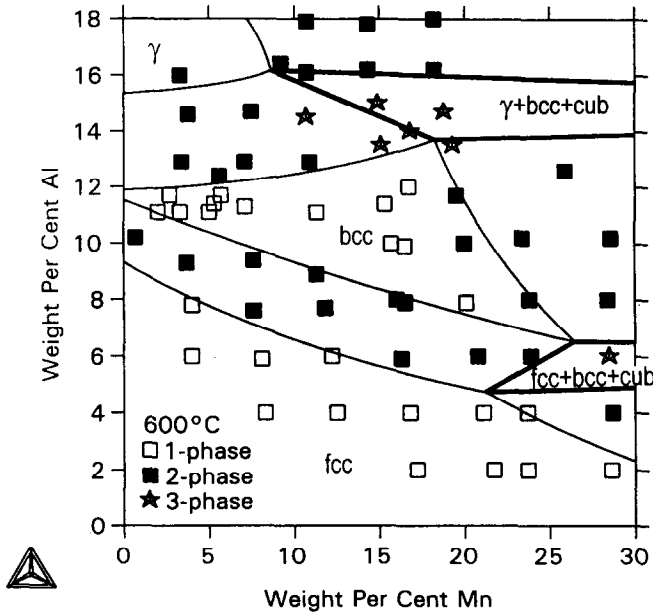


FIG.7

Calculated isothermal section in the copper-rich part of the Cu-Al-Mn system at 600°C, together with experimental data points [56Wes].

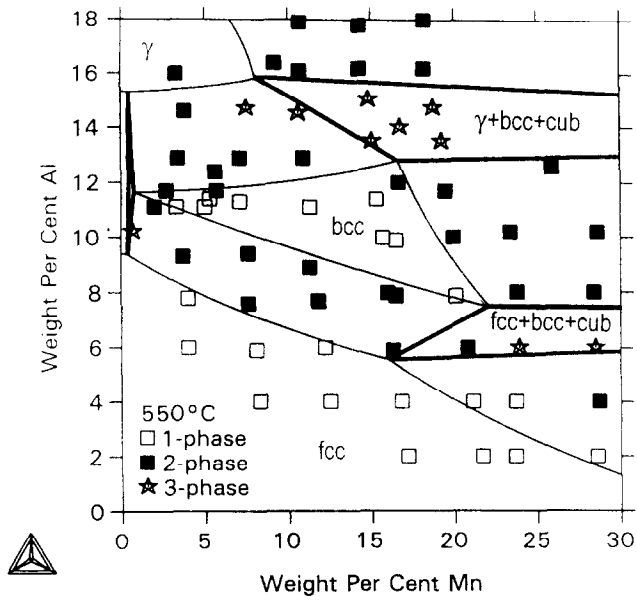


FIG.8

Calculated isothermal section in the copper-rich part of the Cu-Al-Mn system at 550°C, together with experimental data points [56Wes].

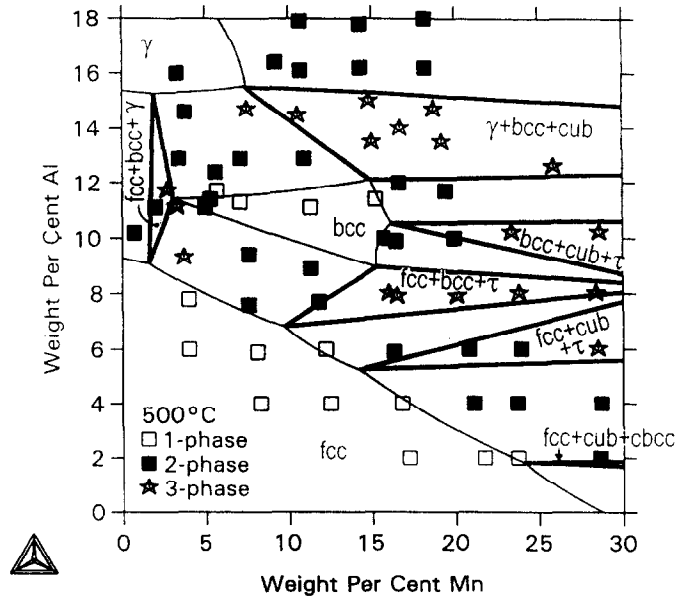


FIG.9

Calculated isothermal section in the copper-rich part of the Cu-Al-Mn system at 500°C, together with experimental data points [56Wes].

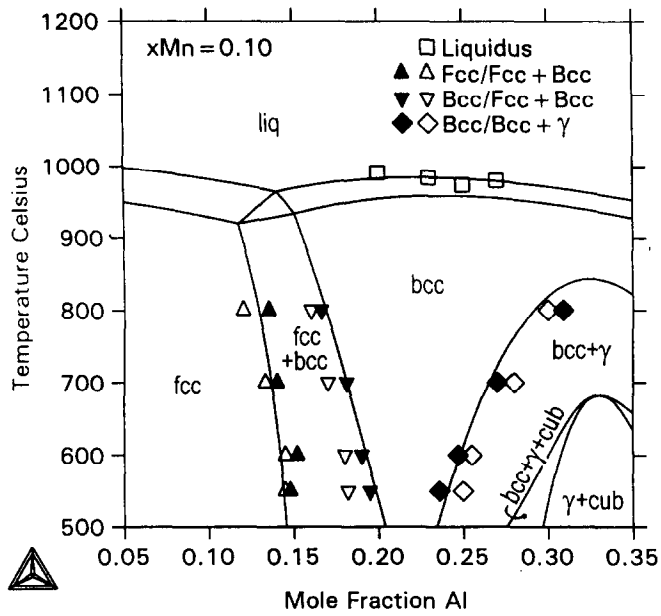


FIG.10

Calculated isopleth at  $x_{Mn}=0.10$  in the copper-rich part of the Cu-Al-Mn system, together with experimental data points [56Wes, 98Kai].

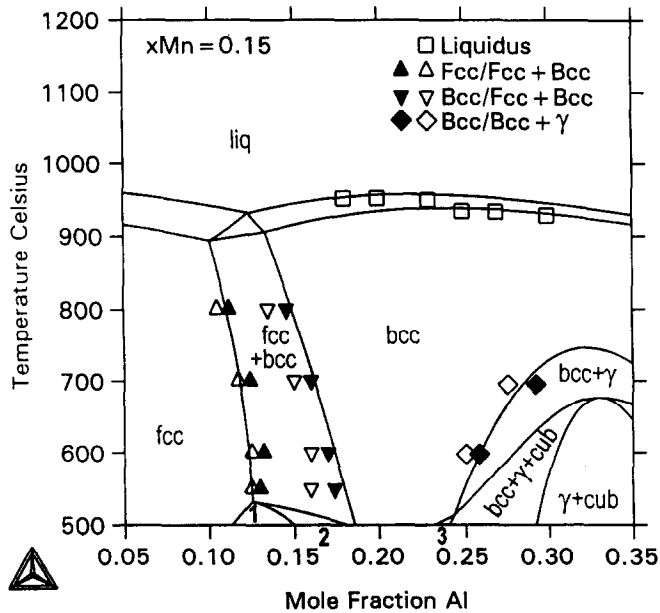


FIG.11

Calculated isopleth at  $x_{Mn}=0.15$  in the copper-rich part of the Cu-Al-Mn system, together with experimental data points [56Wes, 98Kai]. Part of the phase equilibria is described with numbers as 1=fcc+ $\tau$ , 2=fcc+bcc+ $\tau$ , 3=bcc+cub.

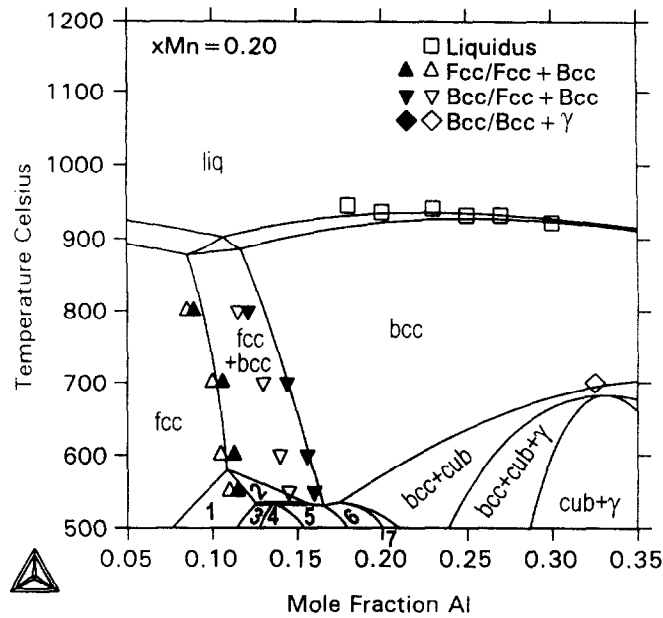


FIG.12

Calculated isopleth at  $x_{Mn}=0.20$  in the copper-rich part of the Cu-Al-Mn system, together with experimental data points [56Wes, 98Kai]. Part of the phase equilibria is described with numbers as 1=fcc+cub, 2=fcc+bcc+cub, 3=fcc+cub+ $\tau$ , 4=fcc+ $\tau$ , 5=fcc+bcc+ $\tau$ , 6=bcc+ $\tau$ , 7=bcc+cub+ $\tau$ .

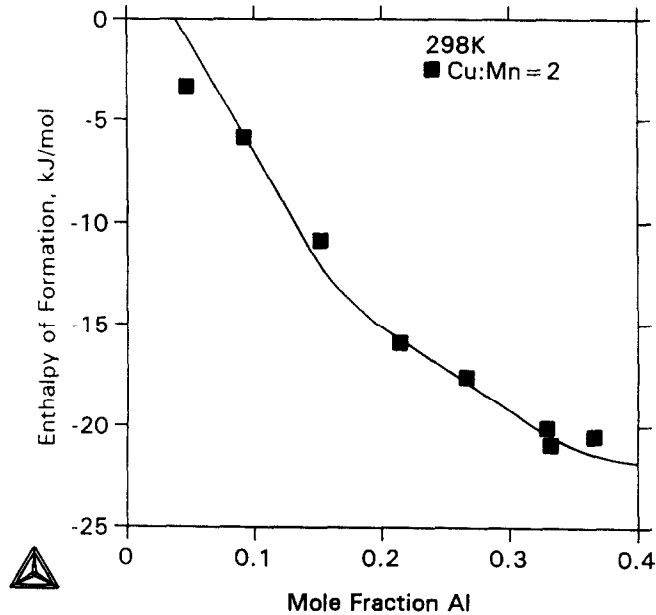


FIG.13

Calculated enthalpy of formation of ternary Cu-Al-Mn alloys at 298K, at a composition ratio of Cu:Mn=2, together with experimental data points [37Kör]. The reference state for copper, aluminum and manganese are pure fcc Cu, pure fcc Al and pure bcc Mn, respectively.